Monthly Notices
of the
ROYAL ASTRONOMICAL SOCIETY

MNRAS **466,** 1848–1856 (2017)
Advance Access publication 2016 December 13

doi:10.1093/mnras/stw3247

Optical photometry and spectroscopy of the low-luminosity, broad-lined Ic supernova iPTF15dld

E. Pian,[1,2★] L. Tomasella,[3] E. Cappellaro,[3] S. Benetti,[3] P. A. Mazzali,[4,5] C. Baltay,[6] M. Branchesi,[7,8] E. Brocato,[9] S. Campana,[10] C. Copperwheat,[4] S. Covino,[10] P. D'Avanzo,[10] N. Ellman,[6] A. Grado,[11] A. Melandri,[10] E. Palazzi,[1] A. Piascik,[4] S. Piranomonte,[9] D. Rabinowitz,[6] G. Raimondo,[12] S. J. Smartt,[13] I. A. Steele,[4] M. Stritzinger,[14] S. Yang,[3] S. Ascenzi,[9] M. Della Valle,[11,15] A. Gal-Yam,[16] F. Getman,[11] G. Greco,[7,8] C. Inserra,[13] E. Kankare,[13] L. Limatola,[11] L. Nicastro,[1] A. Pastorello,[3] L. Pulone,[9] A. Stamerra,[2,17] L. Stella,[9] G. Stratta,[7,8] L. Tartaglia[3] and M. Turatto[3,18]

[1]*INAF, Istituto di Astrofisica Spaziale e Fisica Cosmica di Bologna, Via Gobetti 101, I-40129 Bologna, Italy*
[2]*Scuola Normale Superiore, Piazza dei Cavalieri 7, I-56126 Pisa, Italy*
[3]*INAF, Osservatorio Astronomico di Padova, Vicolo dell'Osservatorio 5, I-35122 Padova, Italy*
[4]*Astrophysics Research Institute, Liverpool John Moores University, IC2, Liverpool Science Park, 146 Brownlow Hill, Liverpool L3 5RF, UK*
[5]*Max-Planck-Institut für Astrophysik, Karl-Schwarzschild-Str. 1, D-85748 Garching, Germany*
[6]*Physics Department, Yale University, PO Box 208120, New Haven, CT 06520, USA*
[7]*Universitá degli Studi di Urbino 'Carlo Bo', Dipartimento di Scienze Pure e Applicate, Piazza della Repubblica 13, I-61029 Urbino, Italy*
[8]*INFN, Sezione di Firenze, I-50019 Sesto Fiorentino, Firenze, Italy*
[9]*INAF, Osservatorio Astronomico di Roma, Via di Frascati, 33, I-00040 Monteporzio Catone, Italy*
[10]*INAF, Osservatorio Astronomico di Brera, Via E. Bianchi 46, I-23807 Merate (LC), Italy*
[11]*INAF, Osservatorio Astronomico di Capodimonte, salita Moiariello 16, I-80131, Napoli, Italy*
[12]*INAF, Osservatorio Astronomico di Teramo, Via M. Maggini s.n.c., I-64100 Teramo, Italy*
[13]*Astrophysics Research Centre, School of Mathematics and Physics, Queen's University Belfast, Belfast BT7 1NN, UK*
[14]*Department of Physics and Astronomy, Aarhus University, Ny Munkegade 120, DK-8000 Aarhus C, Denmark*
[15]*International Center for Relativistic Astrophysics, Piazza delle Repubblica, 10, I-65122 Pescara, Italy*
[16]*Department of Particle Physics and Astrophysics, Weizmann Institute of Science, Rehovot 76100, Israel*
[17]*INAF, Osservatorio Astronomico di Torino, Via Osservatorio 30, I-10025 Torino, Italy*
[18]*Physics & Astronomy Department, Texas Tech University, Lubbock, TX 79409, USA*

Accepted 2016 December 9. Received 2016 December 8; in original form 2016 October 29

ABSTRACT

Core-collapse stripped-envelope supernova (SN) explosions reflect the diversity of physical parameters and evolutionary paths of their massive star progenitors. We have observed the Type Ic SN iPTF15dld ($z = 0.047$), reported by the Palomar Transient Factory. Spectra were taken starting 20 rest-frame days after maximum luminosity and are affected by a young stellar population background. Broad spectral absorption lines associated with the SN are detected over the continuum, similar to those measured for broad-lined, highly energetic SNe Ic. The light curve and maximum luminosity are instead more similar to those of low luminosity, narrow-lined Ic SNe. This suggests a behaviour whereby certain highly stripped-envelope SNe do not produce a large amount of ^{56}Ni, but the explosion is sufficiently energetic that a large fraction of the ejecta is accelerated to higher than usual velocities. We estimate SN iPTF15dld had a main-sequence progenitor of 20–25 $M_{\odot}$, produced a ^{56}Ni mass of $\sim$0.1–0.2 $M_{\odot}$, had an ejecta mass of [2–10] $M_{\odot}$, and a kinetic energy of [1–18] $\times$ 10^{51} erg.

Key words: stars: massive – supernovae: individual: iPTF15dld (LSQ15bfp, PS15clr) – galaxies: starburst.

★ E-mail: elena.pian@sns.it

1 INTRODUCTION

Stripped-envelope supernovae (SNe), i.e. core-collapse SNe that have lost their hydrogen envelope, and retained (Type Ib) or lost (Type Ic) their helium envelope, are the progeny of massive stars (Nomoto & Hashimoto 1988; Heger et al. 2003). Their light curves (Brown et al. 2009; Drout et al. 2011; Li et al. 2011; Bianco et al. 2014; Pritchard et al. 2014; Taddia et al. 2015; Lyman et al. 2016; Prentice et al. 2016) and spectra (Filippenko 1997; Matheson et al. 2001; Modjaz et al. 2014, 2016) display significant diversity, owing to the many different parameters of the exploding stellar cores (masses, rotation rates, metallicity, multiplicity), and possibly to the different degree of asphericity of the explosion (Wheeler et al. 2000).

Type Ic SNe characterized by broad absorption lines or high photospheric velocities (∼15 000–20 000 km s^{-1} at maximum luminosity), and hence high kinetic energies (∼10^{52} erg), accompany the majority of long-duration gamma-ray bursts (GRBs; Woosley & Bloom 2006). This points to the presence of an extra source of energy, besides radioactive ^{56}Ni, i.e. a rotating, and possibly accreting, inner compact remnant. This 'engine' may play a role also in ∼5 per cent of all detected SNe Ic with high photospheric velocities, which are however not accompanied by GRBs (Mazzali et al. 2002; Valenti et al. 2008a; Soderberg et al. 2010; Corsi et al. 2011; Pignata et al. 2011).

This heterogeneous phenomenology needs to be mapped on to the properties of the progenitors and the explosions, and the intrinsic physical effects must be distinguished from those generated by differences in the viewing angle towards the explosion symmetry axis. Therefore, it is important to observe these SNe accurately and to build a complete physical scenario. Optical multicolour searches with very large field-of-view cameras and high cadence are ideal to detect a large number of core-collapse SNe, which are rather common, but often faint and buried in their host galaxy's starlight. During the wide field optical searches of the huge sky localization uncertainty area of the gravitational wave candidate detected by the advanced LIGO interferometers (aLIGO; Abbott et al. 2016) on 2015 October 22 (called G194575; LIGO Scientific Collaboration and Virgo 2015) and subsequently flagged as a low-probability event (false alarm rate of 1/1.5 per days; LIGO Scientific Collaboration and Virgo 2016), many multiwavelength transients were detected that are unrelated with the event (see Corsi et al. 2016; Palliyaguru et al. 2016, and references therein), a fraction of which were spectroscopically classified. Among these is iPTF15dld.

SN iPTF15dld was detected (Singer et al. 2015) by the 48 inch Oschin telescope at Mount Palomar during the intermediate Palomar Transient Factory (PTF) survey (Law et al. 2009; Rau et al. 2009; Kulkarni 2013) on October 23, 08:15 UT at coordinates RA = $00^{h}58^{m}13\overset{s}{.}28$, Dec = $-03^{\circ}39'50\overset{''}{.}3$ with a magnitude of 18.50 (Mould *R* filter, AB system; Ofek et al. 2012). The initial identification as a Seyfert 2 galaxy at $z = 0.046$ (Tomasella et al. 2015a), based on a preliminary spectral analysis, was later revised to the classification as a broad-lined Type Ic SN (Benetti et al. 2015). We here very slightly revise the redshift to $z = 0.047$ based on accurate analysis of the host galaxy emission lines. This corresponds to a distance of 200 Mpc using $H_0 = 73$ km s^{-1} Mpc^{-1} (Riess et al. 2016) and a flat cosmology with $\Omega_m = 0.31$ (Planck Collaboration XIII 2016). The Galactic extinction along the SN line of sight is $A_V = 0.085$ mag (Schlafly & Finkbeiner 2011). The SN was also independently discovered as LSQ15bfp on 2015 October 5 with $V = 19.5$ mag during the La Silla QUEST survey (LSQ; Baltay et al. 2013; Walker et al. 2015) by Rabinowitz et al. (2015), who also report a pre-discovery detection on 2015 October 3 at $V = 20.2$ mag and a brightening of 0.7 mag in 2 d suggesting that this date must be very close to explosion time. The object was also detected by Pan-STARRS as PS15crl in six separate exposures on 2015 October 23 (see Smartt et al. 2016 and Huber et al. 2015 for a description of the current Pan-STARRS surveys[1]). The Pan-STARRS reference images show a very blue starburst region that is superimposed on a larger spiral galaxy. Corsi et al. (2016), who reported early optical photometry and a spectrum on 2015 November 7, detected no significant X-ray or radio emission for this SN (see also Evans et al. 2015, 2016).

Here, we present the *Swift*/UVOT and ground-based optical observations of the SN, including those preliminarily reported in Tomasella et al. (2015b) and Steele, Copperwheat & Piascik (2015), and additional spectra acquired within the PESSTO program (Smartt et al. 2015). We adopt 2015 October 3 as the date of explosion, with an uncertainty of 1 d.

2 OBSERVATIONS AND DATA ANALYSIS

Optical photometry and spectroscopy of the SN were acquired at the 1.82 m Copernico telescope at Cima Ekar (Asiago, Italy), at the Telescopio Nazionale Galileo (TNG), Nordic Optical Telescope (NOT) and Liverpool Telescope (LT; Steele et al. 2004) at the Canary Islands (Spain), at the ESO NTT and 1 m Schmidt telescope as part of the PESSTO (Public ESO Spectroscopic Survey for Transient Objects) and LSQ surveys, respectively. UV photometry was taken with the UVOT instrument onboard the *Swift* satellite. The logs of optical photometric and spectroscopic observations are reported in Tables 1 and 2, respectively. The exposure times were typically 5–10 min for the photometry and 20–40 min for spectroscopy. These data were reduced following standard tasks within the IRAF[2] reduction package.

2.1 Photometry

The *r*-band image of the SN field obtained at the Copernico telescope is presented in Fig. 1. The SN exploded in the outskirts of a spiral galaxy, in a starburst region that is marginally resolved both in our and in the SDSS images (∼2.5 arcsec angular size) and contaminates dramatically the measurements of the SN in the bluer bands (see Section 3.1).

Given the complex background, the SN magnitudes were measured via template subtraction. For this purpose, we used the SNOOPY package[3] developed by one of us (EC): this is a collection of PYTHON scripts based on publicly available tools. In particular, for template subtraction we used the 'HOTPANTS package.[4] For the LSQ observations, we used images of the field taken by the LSQ in 2012 as subtraction templates; while for the *ugriz* photometry we used SDSS images, which provide a solid estimate of the pre-explosion background. SN magnitudes in the template-subtracted images were measured by point spread function (PSF) fitting. We found that PSF fitting is less sensitive to background fluctuations compared with

[1] http://star.pst.qub.ac.uk/ps1threepi/

[2] IRAF is distributed by the National Optical Astronomy Observatory, which is operated by the Association of Universities for Research in Astronomy (AURA) under a cooperative agreement with the National Science Foundation.

[3] SNOOPY: a package for SN photometry, http://sngroup.oapd.inaf.it/snoopy.html.

[4] http://www.astro.washington.edu/users/becker/v2.0/hotpants.html

Table 1. Ground-based photometry[a] of iPTF15dld.

MJD	UT	Tel.+instr./Survey	*r*	*i*
57284.17	2015 Sep 19.17	LSQ[b]	>18.8	–
57298.29	2015 Oct 3.29	LSQ	20.2 ± 0.4	–
57300.20	2015 Oct 5.20	LSQ	19.0 ± 0.4	–
57306.17	2015 Oct 11.17	LSQ	18.4 ± 0.4	–
57312.16	2015 Oct 17.16	LSQ	18.4 ± 0.3	–
57318.17	2015 Oct 23.17	LSQ	19.4 ± 0.5	–
57318.98	2015 Oct 23.98	PS[c]	–	18.80 ± 0.04
57319.15	2015 Oct 24.15	LSQ	19.2 ± 0.4	–
57324.13	2015 Oct 29.13	LSQ	20.1 ± 0.5	–
57330.94	2015 Nov 4.94	1.82 m+AFOSC	19.9 ± 0.1	19.9 ± 0.2
57332.11	2015 Nov 6.11	LSQ	20.5 ± 0.4	–
57332.87	2015 Nov 6.87	1.82 m+AFOSC	20.2 ± 0.09	20.5 ± 0.2
57332.92	2015 Nov 6.92	TNG+LRS	20.0 ± 0.1	–
57333.85	2015 Nov 7.85	1.82 m+AFOSC	19.9 ± 0.2	20.4 ± 0.1
57334.10	2015 Nov 8.10	LSQ	20.6 ± 0.4	–
57334.87	2015 Nov 8.87	1.82 m+AFOSC	20.0 ± 0.2	20.4 ± 0.1
57338.84	2015 Nov 12.84	1.82 m+AFOSC	20.1 ± 0.2	20.7 ± 0.3
57341.92	2015 Nov 15.92	1.82 m+AFOSC	20.3 ± 0.2	20.8 ± 0.4
57342.85	2015 Nov 16.85	1.82 m+AFOSC	20.4 ± 0.2	20.8 ± 0.2
57344.90	2015 Nov 18.90	1.82 m+AFOSC	20.5 ± 0.2	21.1 ± 0.3
57358.82	2015 Dec 2.82	1.82 m+AFOSC	20.6 ± 0.2	21.1 ± 0.3
57361.83	2015 Dec 5.83	1.82 m+AFOSC	20.8 ± 0.3	>21.1
57363.83	2015 Dec 7.83	1.82 m+AFOSC	20.5 ± 0.3	>20.7
57366.77	2015 Dec 10.77	1.82 m+AFOSC	20.7 ± 0.1	21.5 ± 0.2
57373.76	2015 Dec 17.76	1.82 m+AFOSC	21.0 ± 0.2	21.5 ± 0.3
57374.72	2015 Dec 18.72	1.82 m+AFOSC	20.8 ± 0.2	>21.1
57399.83	2016 Jan 12.83	NOT+ALFOSC	21.1 ± 0.1	21.9 ± 0.3

Notes. [a]The magnitudes are galaxy subtracted and not corrected for Galactic extinction.
[b]The La Silla QUEST survey uses the 1 m ESO Schmidt telescope at the La Silla Observatory with the 10 square degree CCD camera.
[c]This value was reported in Rabinowitz et al. (2015) from the Pan-STARRS Survey for Transients (Huber et al. 2015).

Table 2. Ground-based spectroscopy of iPTF15dld.

MJD	UT	Phase[a]	Telescope	Instrument	grism
57330	2015 Nov 4	19.1	1.82m	AFOSC	gm4
57332	2015 Nov 6	21.0	TNG	LRS	LRS-B
57332	2015 Nov 6	21.0	LT	SPRAT	Red
57333	2015 Nov 7	22.0	NTT	EFOSC2	gr13
57342	2015 Nov 16	30.6	1.82m	AFOSC	gm4
57344	2015 Nov 18	32.5	1.82m	AFOSC	gm4
57360	2015 Dec 4	47.8	NTT	EFOSC2	gr13
57373	2015 Dec 17	60.2	LT	SPRAT	Red
57374	2015 Dec 18	61.2	LT	SPRAT	Red

Note. [a]Phase is given in days with respect to light-curve maximum and in rest frame.

standard aperture photometry. The LSQ images are unfiltered, but close to the *r* filter, therefore the magnitudes resulting from the photometry were converted to this band using a calibrating sequence of field stars.

Starting on 2015 November 6.97 UT and ending on 2015 November 7.43 UT, the *Swift* satellite observed the target (see observing log in Table 3). The UVOT camera measurements in the optical and UV were reduced according to Brown et al. (2015) and calibrated following Poole et al. (2008) and Breeveld et al. (2010). Aperture photometry with a radius of 5 arcsec with background estimated from a nearby sky area yielded the magnitudes reported in Table 3.

2.2 Spectroscopy

After bias and flat-field correction, the SN spectra were extracted and wavelength calibrated through the use of arc lamp spectra. Flux calibration was derived from observations of spectrophotometric standard stars obtained, when possible, on the same night as the SN. Corrections for the telluric absorption bands were derived using telluric standards. In some cases, non-perfect removal can affect the SN features that overlap with the strongest atmospheric features, in particular with the telluric O2 A band at 7590–7650 Å.

In order to subtract the starburst contribution from the SN spectra, we used the template spectra of star-forming galaxies by Kinney et al. (1996). The best-fitting template was chosen by matching the colours of the starburst region as measured on the pre-explosion SDSS images (Table 4): this indicated a preference for a template with moderate intrinsic absorption ($0.11 < E(B-V) < 0.21$; Kinney et al. 1996), as independently indicated also by the UVOT detections in the UV filters. The spectral template was fitted with a low-order polynomial (to reduce noise in subtraction); the relative contributions of the starburst and SN components were then determined based on the starburst archival magnitudes and on the template-subtracted SN photometry simultaneous with the spectra, respectively. Finally, the template was reduced to the SN redshift and subtracted from the SN spectra in rest frame. With this procedure, the spectra show some variation in the residual continuum of the blue spectral region, which we attribute to uncertainties in the flux calibration. We allowed for a small adjustment in the template continuum slope (corresponding to ±0.1 mag variation in $E(B-V)$) to ensure all spectra show a similar overall continuum.

3 RESULTS

3.1 Host galaxy

The SN is hosted by a compact starburst galaxy/region that, in turn, appears projected over the disc of a spiral galaxy. The narrow emission lines we detected in our spectra (see Section 3.3) indicate that the two objects, starburst and spiral galaxy, are located at the same redshift, although we cannot assess whether they form a unique structure or a galaxy pair. The starburst nucleus is a luminous UV source that was detected by *GALEX* on 2008 October 8 (*GALEX* source J005813.0−033946) with AB magnitudes FUV = 18.89, and NUV = 18.38, (Kron aperture; note that the NUV band, ∼2300 Å, is similar to the *uvm2* band of *Swift*/UVOT).

The SDSS magnitudes of the starburst region at the location of the SN are reported in Table 4. Note that the half-magnitude offset in the measurements obtained with different photometric apertures does not affect significantly the colours. The *u*-band magnitude obtained with the 5 arcsec radius aperture, $u = 19.1$ mag, is consistent with the AB magnitude measured by UVOT in the *U* band (Table 3). This and the lack of UV flux variability suggest that the source detected by UVOT is dominated by the emission of the starburst region, so that the UV emission of the SN is undetectable. At a distance of 200 Mpc, the starburst component has an absolute magnitude in the *g* band of −18.5 mag, which places it at the bright end of the blue compact dwarf luminosity function (Tolstoy, Hill & Tosi 2009).

Fig. 2 shows a stellar population synthesis model to estimate the age of the stellar population in the vicinity of the SN from the observed colours (Brocato et al. 2000; Raimondo 2009). The model assumes solar metallicity and ages comprised between 1 and 500 Myr. By correcting the starburst colours – adopting the circumstellar Large Magellanic Cloud extinction law of Goobar

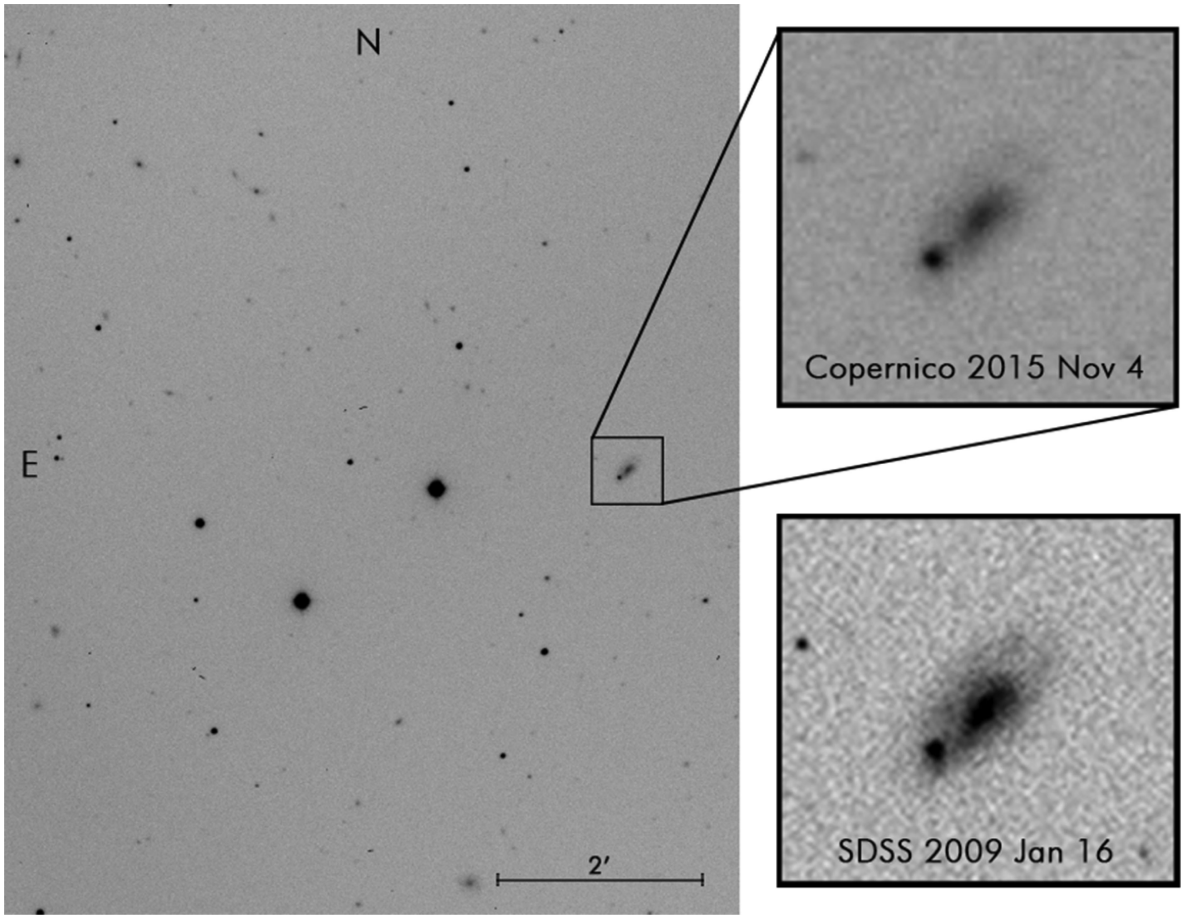

Figure 1. Images of the field of iPTF15dld in the *r* band (exposure time of 120 s) taken on 2015 November 4 with the 1.82 m Copernico telescope (larger panel on the left and enlargement centred on the host galaxy on the top-right smaller panel) and from the SDSS prior to explosion (smaller bottom-right panel, covering the same area as the small top-right panel).

Table 3. *Swift*/UVOT observations of the region of iPTF15dld on 2015 November 6–7[a].

Filter	Expotime (s)	Vega mag[b]	AB mag[b]
v	508.36	17.82 ± 0.08 (stat) ± 0.01 (sys)	17.81 ± 0.08 (stat) ± 0.01 (sys)
b	706.64	18.24 ± 0.05 (stat) ± 0.02 (sys)	18.12 ± 0.05 (stat) ± 0.02 (sys)
u	706.65	17.72 ± 0.05 (stat) ± 0.02 (sys)	18.74 ± 0.05 (stat) ± 0.02 (sys)
*uvw*1	1415.24	17.55 ± 0.04 (stat) ± 0.03 (sys)	19.08 ± 0.04 (stat) ± 0.03 (sys)
*uvm*2	2576.14	17.51 ± 0.03 (stat) ± 0.03 (sys)	19.10 ± 0.03 (stat) ± 0.03 (sys)
*uvw*2	2576.14	17.51 ± 0.03 (stat) ± 0.03 (sys)	19.20 ± 0.03 (stat) ± 0.03 (sys)

Notes. [a]Note that these measurements refer entirely to the emission of the starburst region underlying the SN, while the SN itself is undetected at these wavelengths.
[b]Not corrected for Galactic extinction.

Table 4. Magnitudes[a] of the starburst region.

Filter[a]	5 arcsec radius	3 arcsec radius
u	19.09	19.60
g	18.03	18.59
r	17.77	18.43
i	17.50	18.26
z	17.46	18.22

Note. [a]In the SDSS system, not corrected for Galactic extinction.

(2008) as in Brown et al. (2010) – for moderate values of intrinsic extinction (from null to $E(B-V) = 0.35$, i.e. somewhat higher than the maximum intrinsic extinction of the assumed star-forming galaxy template, $E(B-V) = 0.21$), in addition to the Galactic one ($E(B-V) = 0.027$), we obtain the intrinsic colours reported in Fig. 2 as filled blue squares. The colour resulting from maximum correction is consistent with a population age of 10 Myr, which corresponds to the evolution time of a 20 $M_{\odot}$ star. The use of an extinction curve more suitable for hot stars (Siegel et al. 2014) leads to a similar conclusion.

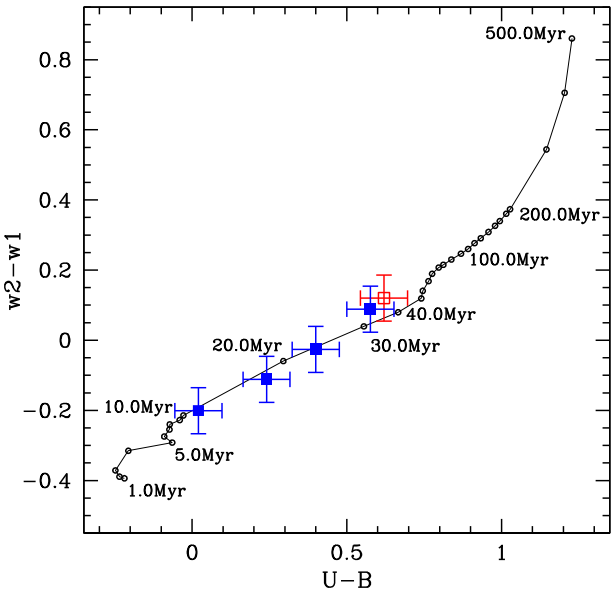

Figure 2. Stellar synthesis diagram for the starburst region underlying iPTF15dld. Ages of the stellar populations along the diagram are indicated. The squares represent the observed (open red) and de-reddened (filled blue) colours of the starburst, obtained from the magnitudes reported in Table 3 by correcting for different amounts of internal absorption ($E(B-V) = 0.027$, 0.137, 0.237, 0.377 mag) and using the circumstellar Large Magellanic Cloud extinction law with no red-tail-corrected coefficients of Brown et al. (2010; see their table 1). For maximum extinction ($E(B-V) = 0.377$ mag), the starburst is compatible with an age of 10 Myr, equivalent to the lifetime of a 20 $M_\odot$ star.

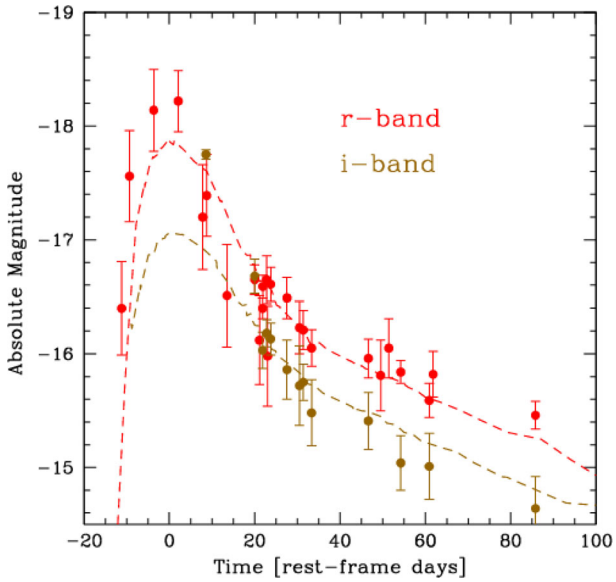

Figure 3. Light curves of iPTF15dld in the r band (red circles) and the i band (brown circles), corrected for Galactic extinction ($A_V = 0.085$). At $z = 0.047$, the central wavelengths of these bands correspond to 5980 and 7328 Å, respectively. The time origin corresponds to the maximum of the r-band light curve. For comparison, we overlaid the light curves of the Type Ic SN 2007gr at identical reference wavelengths (dashed curves; see text for the construction of these templates). The 'r-band'-equivalent template of SN 2007gr was brightened by 0.7 mag for best match with iPTF15dld.

This satisfactory match indicates the presence of a young massive star population, consistent with the explosion of a massive stellar core that has evolved from a main-sequence mass of ∼20 $M_\odot$ (see Section 4). We note that a Milky Way extinction curve only provides a match with the starburst colours if the intrinsic extinction is as high as $E(B-V) = 0.8$, which is inconsistent with the observed colours of the starburst and indicates that this region presents the characteristics of a more rapidly star forming, lower metallicity, less evolved environment than our Galaxy. In fact, the star formation rate of ∼1 $M_\odot$ yr^{-1} derived by Palliyaguru et al. (2016) from radio excess detection within a region a few kpc across, spatially compatible with the UVOT source, points to an explosion site of high star formation rate per unit mass. This is typical for stripped-envelope SNe (Anderson et al. 2012; Crowther 2013), expected to be predominantly associated with bright regions of massive and rapid star formation, which could make their detection systematically more arduous at large distances even with the biggest telescopes.

3.2 Light curves

The r- and i-band magnitudes of the point-like SN source, derived with PSF fitting from the background-subtracted images (see Section 2.1), are reported in Table 1 and, after correction for Galactic absorption (using $A_V = 0.085$; Schlafly & Finkbeiner 2011, and the extinction curve of Cardelli, Clayton & Mathis 1989), in Fig. 3. We have not corrected for intrinsic extinction within the starburst region because we cannot estimate how much this influences the SN emission (it depends on the relative position of the SN and starburst with respect to the observer) and we have no evidence that iPTF15dld is significantly absorbed in its rest frame. In fact, its $R-I$ colour, computed from the r- and i-band light curves, is comparable to that of well-monitored SNe Ic close to maximum luminosity (Richmond et al. 1996; Galama et al. 1998; Patat et al. 2001; Foley et al. 2003; Ferrero et al. 2006; Taubenberger et al. 2006; Valenti et al. 2008a,b; Hunter et al. 2009), and possibly bluer at later times, likely owing to significant background still affecting the weaker r-band flux. No detection of iPTF15dld was obtained with the ugz filters in individual exposures. The magnitudes from the co-added exposures in these filters are consistent with the SDSS measurements.

The r- and i-band light curves of iPTF15dld were compared with those of SN 2007gr, a type Ic SN of 'classical' spectral appearance, i.e. with no broad absorption lines (Valenti et al. 2008b; Hunter et al. 2009). At $z = 0.047$, the central wavelengths of the r- and i-band filters correspond to 5980 and 7328 Å, respectively. From the VRI light curves of SN 2007gr we have constructed template light curves at those two reference wavelengths and reported them in Fig. 3, after brightening the template at 5980 Å by 0.7 mag. With the exception of the first i-band point, which is significantly brighter, the match with the templates is generally satisfactory, and it indicates that iPTF15dld is a factor of ∼2 brighter at ∼6000 Å and therefore bluer than SN 2007gr in the 6000–8000 Å range.

Although the available photometry (r and i bands only) is not sufficient to construct a proper pseudo-bolometric light curve, the total spectral flux is a rough proxy of the bolometric behaviour. For each spectrum, we integrated the flux calibrated, dereddened spectral signal in the rest frame, approximately corresponding to the range 3800–7800 Å (see Fig. 5) and obtained a bolometric light curve that is similar in shape to those of the faintest stripped-envelope SNe that were monitored long enough to allow a comparison with iPTF15dld (SNe 1994I, 2002ap) and in particular to that of SN 2007gr (see Hunter et al. 2009). Since our pseudo-bolometric estimate does not include the near-UV and near-infrared contributions, we have estimated this using other SNe Ic that have good photometric coverage in these bands simultaneous with the optical. At epochs

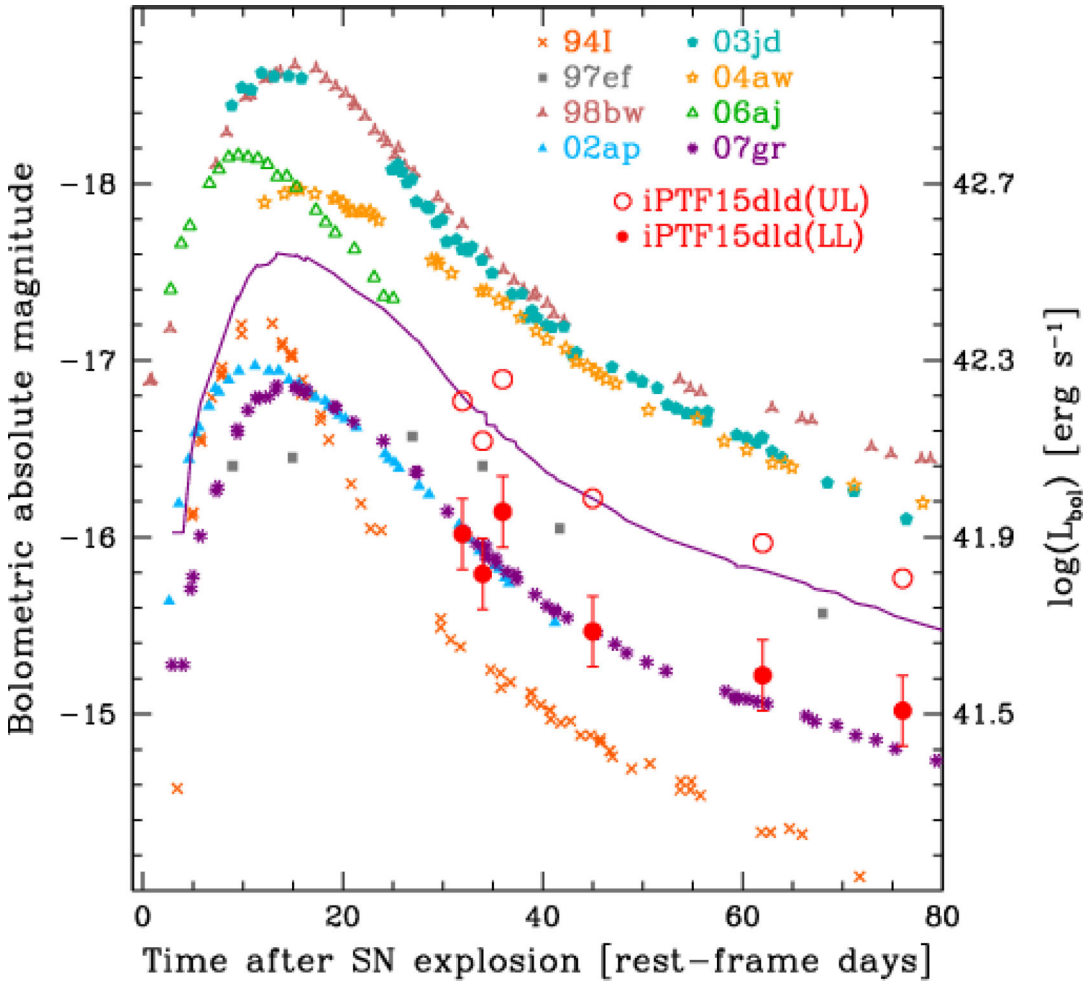

Figure 4. Pseudo-bolometric (UVOIR) light curves of stripped-envelope SNe. The curve of iPTF15dld was obtained by integrating the spectral flux in its rest frame (filled red points). Since this covers a limited wavelength range (∼3800–7800 Å), it is likely a lower limit (LL) on the UVOIR light curve, and a correction of a factor of 2 was applied to take into account the flux in a broader range (3300–24 000 Å), based on the ratio of broad-band optical and near-infrared fluxes in SNe 1998bw, 2004aw, 2007gr. These corrected pseudo-bolometric luminosities, that can be considered an upper limit (UL) on the UVOIR light curve, are reported as open red circles. The errors on the iPTF15dld luminosities are estimated to be ∼20 per cent. For clarity, the errors on the bolometric luminosities of all other SNe were omitted (the data for these are from Iwamoto et al. 2000; Ferrero et al. 2006; Hunter et al. 2009, and references therein; the data of SN 1997ef were corrected for the different value of the Hubble constant adopted here). The purple curve represents the bolometric light curve of SN 2007gr brightened by 0.75 mag.

comparable to those of the iPTF15dld photometry, the near-UV and near-infrared fluxes of type SNe Ic combined represent about 40–50 per cent of the total flux in 3000–24000 Å (e.g. SN 1998bw, Patat et al. 2001; SN 2004aw, Taubenberger et al. 2006; SN 2007gr, Hunter et al. 2009). Even taking this into account, iPTF15dld is still less luminous than the average of stripped-envelope SNe (Fig. 4).

3.3 Spectra

The two spectra taken at the 1.82 m Copernico telescope on 2015 November 16 and 18 were averaged, owing to their closeness in time and similarity, and so were the two spectra acquired at the LT with SPRAT on 2015 December 17 and 18. Six final spectra, corrected for Galactic extinction and redshift, are reported in Fig. 5. The SPRAT spectrum of November 6 was not shown because it is very close in time to the TNG spectrum and of lower signal-to-noise ratio. The starburst dominates the spectral emission with a blue continuum and narrow emission lines. However, when its contribution is removed (see Section 2.2), the broad lines typical of SNe Ic become visible in the visual/red spectral regions. Neither hydrogen nor helium absorption lines are seen, indicating a high degree of envelope stripping and leading to Type Ic classification of the SN. The narrow emission lines from the underlying starburst region were removed.

In search of a close spectral analogue of iPTF15dld, we compared its spectra with those of eight Type Ic SNe, both broad- and narrow-lined (SN 1994I, Filippenko et al. 1995; Richmond et al. 1996; Millard et al. 1999; SN 1997ef, Iwamoto et al. 2000; Mazzali et al. 2000; SN 1998bw, Patat et al. 2001; SN 2002ap, Gal-Yam, Ofek & Shemmer 2002; Mazzali et al. 2002; Foley et al. 2003; SN 2003jd, Valenti et al. 2008a; SN 2004aw, Taubenberger et al. 2006; SN 2006aj, Mazzali et al. 2006; SN 2007gr, Hunter et al. 2009). With the partial aid of a χ^2-minimization routine, we selected the spectra of our SN templates that best matched, in the 4000–7500 Å wavelength range, those of iPTF15dld at comparable phases after light curve maximum.

SNe 1998bw and 2006aj, which were associated with GRBs (Galama et al. 1998; Pian et al. 2000, 2006; Campana et al. 2006), do

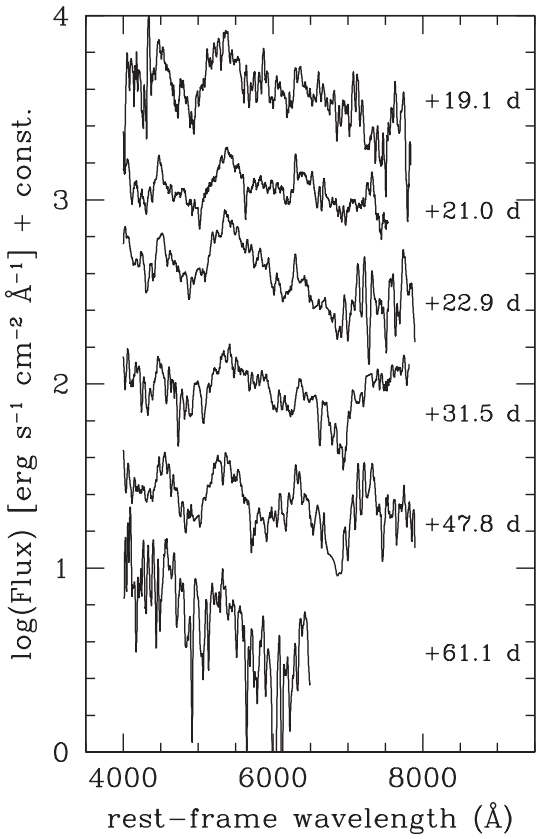

Figure 5. Spectra of iPTF15dld in rest frame, corrected for Galactic extinction ($A_V = 0.085$), smoothed with a boxcar of 50 Å and arbitrarily scaled in flux. The phases are given in rest frame, with respect to maximum luminosity.

not compare well with iPTF15dld because their spectra have significantly broader absorption lines (although in the case of SN2006aj, only one spectrum overlaps in phase). On the other hand, the classical SNe 1994I and 2007gr represent an equally unsatisfactory match because they have narrower lines than our target. The first four spectra of iPTF15dld are more similar to those of SNe 1997ef, 2002ap, 2003jd and 2004aw, that are broad-lined Ic SNe with no accompanying GRB (see also Corsi et al. 2016). These have kinetic energies higher than seen on average in SNe Ic, although they are neither as massive nor as luminous as GRB SNe. The last spectra (2015 December) resemble both broad- and narrow-lined Ic SN spectra, presumably because they are more noisy and at those epochs (∼50–60 rest-frame days after maximum), the photospheric velocities have significantly decreased also in broad-lined SNe. In Figs 6 and 7, we show two examples of spectral comparison.

While the signal-to-noise ratio of the spectra and the partial blending of absorption lines, due to their width, makes it difficult to isolate the chemical species and measure their associated velocities, the similarity with broad-lined SNe suggests higher than normal photospheric velocities.

4 DISCUSSION

The light curve of iPTF15dld resembles that of normal, narrow-lined Type Ic SNe, with SN 2007gr (Hunter et al. 2009) providing an excellent match (Fig. 3). However, the photospheric absorption lines are broad, so this is classified as a broad-lined Ic SN, rather similar to well-monitored broad-lined SNe Ic at comparable epochs

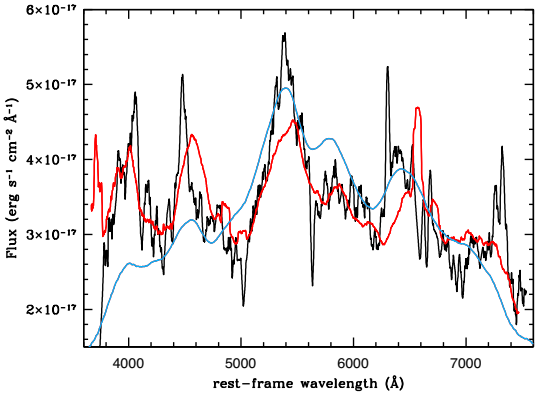

Figure 6. Spectrum of iPTF15dld of 2015 November 6 (black) dereddened with $A_V = 0.085$ compared with those of SN 1997ef (red) and SN 1998bw (blue) at comparable rest-frame phases. The spectrum of SN 1998bw was dereddened with $A_V = 0.16$, while that of SN 1997ef needs no absorption correction. All spectra were smoothed with a boxcar of 50 Å. The absorption lines of SN 1998bw are significantly broader than those of iPTF15dld, while those of SN 1997ef represent a better match.

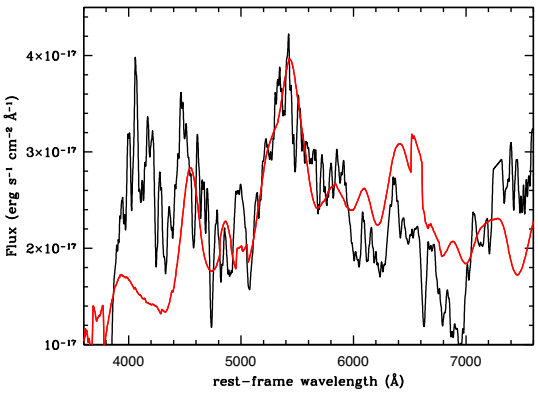

Figure 7. Spectrum of iPTF15dld of 2015 November 17 (black) dereddened with $A_V = 0.085$ compared with that of SN 2003jd (red) at comparable rest-frame phase, dereddened with $A_V = 0.43$. All spectra were smoothed with a boxcar of 50 Å.

after light maximum (SNe 1997ef, 2002ap, 2003jd, 2004aw). Since spectra were taken only starting 20 d after maximum, we cannot make an assessment of the photospheric velocity before and around maximum; similarly, the photometric information does not allow us to construct a pseudo-bolometric light curve covering the epoch of maximum luminosity. As a consequence, our estimates of the physical parameters are only approximated.

In the absence of synthetic light curve and spectra based on a detailed radiative transfer model obtained from observed quantities, the basic SN physical parameters can be derived by rescaling those of other well-studied SNe using the fundamental relationships of Arnett (1982), as done for instance in Corsi et al. (2012), Mazzali et al. (2013), Walker et al. (2014) and D'Elia et al. (2015). However, iPTF15dld lacks an estimate of both its light curve width, τ, and its photospheric velocity at maximum luminosity, $v_{\rm ph}$. Therefore, our estimate of its kinetic energy and ejecta mass can only be based on an average of these parameters for the five SNe that provide the best light curve and spectral match (see Section 3.3).

From the physical parameters estimated for SNe 1997ef, 2002ap, 2003jd, 2004aw and 2007gr, (Iwamoto et al. 2000; Mazzali et al. 2000, 2002; Taubenberger et al. 2006; Valenti et al. 2008a;

Hunter et al. 2009), we derive ranges of [1–18] $\times$ 10^{51} erg and [2–10] $M_{\odot}$ for the kinetic energy and ejecta mass of iPTF15dld, respectively. Since the shape and luminosity of the bolometric light curve suggest that iPTF15dld could have been similar to SN 2007gr or up to a factor of 2 more luminous at peak, we accordingly estimate that the mass of radioactive ^{56}Ni synthesized in the explosion may be in the interval [0.08–0.2] $M_{\odot}$. These values are consistent with a progenitor of main-sequence mass of the order of $\sim$20–25 $M_{\odot}$. A dedicated accurate model is not completely justified by the limited quality of these data.

Broad-lined Ic SNe of modest luminosity are a rather uncommon and poorly known class, and have started to be detected in larger numbers thanks to dedicated surveys. As GRB SNe that are significantly more massive and luminous, they may be partially powered by an inner engine, i.e. an unusual type of remnant, like a magnetar or a black hole. The prototype of this sub-class is SN 2002ap (Mazzali et al. 2002) for which evidence had been found of a small fraction of ejected material accelerated to velocities larger than 30 000 km s^{-1}. Since these objects have low ejecta mass (their synthesized ^{56}Ni mass is small), the total kinetic energy is also not extremely large ($\sim 10^{51}$ erg), but the high photospheric velocities suggest a powerful engine. Whether these are the progenitors of GRBs that are misaligned with respect to the line of sight and therefore go undetected, or they represent a population of intermediate properties between classical, narrow-lined SNe Ic and GRB SNe, is matter of controversy (Mazzali et al. 2005; Maeda et al. 2008; Soderberg et al. 2010; Pignata et al. 2011). Clarification of this issue (e.g. through late-epoch radio observations; van Eerten & MacFadyen 2011) may lead to a simplification of the apparent diversity of stripped-envelope SNe. We note that the opposite, i.e. low photospheric velocities in highly luminous SNe are never observed (e.g. Mazzali et al. 2013).

The case of iPTF15dld shows how optical surveys that cover large areas of the sky with good cadence using classical facilities can improve dramatically the study of a broad range of transients. Early detection and decent monitoring of objects with a variety of properties will fill gaps present in the current information and unify seemingly different phenomena.

ACKNOWLEDGEMENTS

We acknowledge data from the Pan-STARRS1 telescope that is supported by NASA under grant no. NNX12AR65G and grant no. NNX14AM74G issued through the NEO Observation Program. We acknowledge funding from ASI INAF grant I/088/06/0, from the Italian Ministry of Education and Research and the Scuola Normale Superiore, and from INAF project: 'Gravitational Wave Astronomy with the first detections of aLIGO and aVIRGO experiments' (PI: E. Brocato). GR is partially supported by the PRIN INAF-2014 'EXCALIBURS: EXtragalactic distance scale CALIBration Using first-Rank Standard candles' (PI: G. Clementini). L. Tomasella, EC and SB are partially supported by the PRIN-INAF 2014 project 'Transient Universe: unveiling new types of stellar explosions with PESSTO'. MS gratefully acknowledges generous support provided by the Danish Agency for Science and Technology and Innovation realized through a Sapere Aude Level 2 grant. MB, GG and GS acknowledge financial support from the Italian Ministry of Education, University and Research (MIUR) through grant FIRB 2012 RBFR12PM1F. We thank the staff of the Copernico telescope, LT, NTT, TNG, NOT and LSQ, in particular W. Boschin, D. Carosati, S. Dalle Ave, L. Di Fabrizio, A. Fiorenzano, P. Ochner, T. Pursimo and T. Reynolds. We are grateful to S. Valenti for sending archival supernova data in digital form, P. Nugent for his support of this project, L. Singer for his critical reading of the manuscript and to our referee for constructive suggestions. This research is based on observations made with the *Copernico* telescope (Asiago, Italy) of INAF - Osservatorio Astronomico di Padova; with the NTT at the European Organization for Astronomical Research in the Southern hemisphere, Chile, as part of the Public ESO Spectroscopic Survey for Transient Objects Survey (PESSTO) ESO programmes 188.D-3003, 191.D-0935; with the Telescopio Nazionale Galileo, operated by the Fundación Galileo Galilei of INAF, with the Liverpool Telescope, operated by Liverpool John Moores University with financial support from the UK Science and Technology Facilities Council, and with the Nordic Optical Telescope, operated by the Nordic Optical Telescope Scientific Association, all three on the island of La Palma at the Spanish Observatorio del Roque de los Muchachos of the Instituto de Astrofísica de Canarias. This research has made use of the Weizmann Interactive Supernova data Repository (http://wiserep.weizmann.ac.il), and it used resources of the National Energy Research Scientific Computing Center, a DOE Office of Science User Facility supported by the Office of Science of the US Department of Energy under Contract No. DE-AC02-05CH11231.

REFERENCES

Abbott B. P. et al., 2016, Phys. Rev. Lett., 116, 131103
Anderson J. P., Habergham S. M., James P. A., Hamuy M., 2012, MNRAS, 424, 1372
Arnett W. D., 1982, ApJ, 253, 785
Baltay C. et al., 2013, PASP, 125, 683
Benetti S. et al., 2015, GCN Circ., 18563
Bianco F. B. et al., 2014, ApJS, 213, 19
Breeveld A. A. et al., 2010, MNRAS, 406, 1687
Brocato E., Castellani V., Poli F. M., Raimondo G., 2000, A&AS, 146, 91
Brown P. J. et al., 2009, AJ, 137, 4517
Brown P. J. et al., 2010, ApJ, 721, 1608
Brown P. J. et al., 2015, ApJ, 805, 74
Campana S. et al., 2006, Nature, 442, 1008
Cardelli J. A., Clayton G. C., Mathis J. S., 1989, ApJ, 345, 245
Corsi A. et al., 2011, ApJ, 741, 76
Corsi A. et al., 2012, ApJ, 747, L5
Corsi A. et al., 2016, ApJ, 830, 42
Crowther P. A., 2013, MNRAS, 428, 1927
D'Elia V. et al., 2015, A&A, 577, A116
Drout M. R. et al., 2011, ApJ, 741, 97
Evans P. A. et al., 2015, GCN Circ., 18569
Evans P. A. et al., 2016, MNRAS, 462, 1591
Ferrero P. et al., 2006, A&A, 457, 857
Filippenko A. V., 1997, ARA&A, 35, 309
Filippenko A. V. et al., 1995, ApJ, 450, L11
Foley R. J. et al., 2003, PASP, 115, 1220
Gal-Yam A., Ofek E. O., Shemmer O., 2002, MNRAS, 332, L73
Galama T. J. et al., 1998, Nature, 395, 670
Goobar A., 2008, ApJ, 686, L103
Heger A., Fryer C. L., Woosley S. E., Langer N., Hartmann D. H., 2003, ApJ, 591, 288
Huber M. et al., 2015, Astron. Telegram, 7153
Hunter D. J. et al., 2009, A&A, 508, 371
Iwamoto K. et al., 2000, ApJ, 534, 660
Kinney A. L., Calzetti D., Bohlin R. C., McQuade K., Storchi-Bergmann T., Schmitt H. R., 1996, ApJ, 467, 38
Kulkarni S. R., 2013, Astron. Telegram, 4807, 1
Law N. M. et al., 2009, PASP, 121, 1395
Li W. et al., 2011, MNRAS, 412, 1441

LIGO Scientific Collaboration and Virgo, 2015, GCN Circ., 18442
LIGO Scientific Collaboration and Virgo, 2016, GCN Circ., 18626
Lyman J. D., Bersier D., James P. A., Mazzali P. A., Eldridge J. J., Fraser M., Pian E., 2016, MNRAS, 457, 328
Maeda K. et al., 2008, Science, 319, 1220
Matheson T., Filippenko A. V., Li W., Leonard D. C., Shields J. C., 2001, AJ, 121, 1648
Mazzali P. A., Iwamoto K., Nomoto K., 2000, ApJ, 545, 407
Mazzali P. A. et al., 2002, ApJ, 572, L61
Mazzali P. A. et al., 2005, Science, 308, 1284
Mazzali P. A. et al., 2006, Nature, 442, 1018
Mazzali P. A., Walker E. S., Pian E., Tanaka M., Corsi A., Hattori T., Gal-Yam A., 2013, MNRAS, 432, 2463
Millard J. et al., 1999, ApJ, 527, 746
Modjaz M. et al., 2014, AJ, 147, 99
Modjaz M., Liu Y. C., Bianco F. B., Graur O., 2016, ApJ, 832, 108
Nomoto K., Hashimoto M., 1988, Phys. Rep., 163, 13
Ofek E. O. et al., 2012, PASP, 124, 62
Palliyaguru N. T. et al., 2016, ApJ, 829, L28
Patat F. et al., 2001, ApJ, 555, 900
Pian E. et al., 2000, ApJ, 536, 778
Pian E. et al., 2006, Nature, 442, 1011
Pignata G. et al., 2011, ApJ, 728, 14
Planck Collaboration XIII, 2016, A&A, 594, A13
Poole T. S. et al., 2008, MNRAS, 383, 627
Prentice S. J. et al., 2016, MNRAS, 458, 2973
Pritchard T. A., Roming P. W. A., Brown P. J., Bayless A. J., Frey L. H., 2014, ApJ, 787, 157
Rabinowitz D. et al., 2015, GCN Circ., 18572
Raimondo G., 2009, ApJ, 700, 1247
Rau A. et al., 2009, PASP, 121, 1334
Richmond M. W. et al., 1996, AJ, 111, 327
Riess A. G. et al., 2016, ApJ, 826, 56
Schlafly E. F., Finkbeiner D. P., 2011, ApJ, 737, 103
Siegel M. H. et al., 2014, AJ, 148, 131
Singer L. P. et al., 2015, GCN Circ., 18497
Smartt S. J. et al., 2015, A&A, 579, A40
Smartt S. J. et al., 2016, MNRAS, 462, 4094
Soderberg A. M. et al., 2010, Nature, 463, 513
Steele I. A. et al., 2004, in Oschmann J. M., Jr Proc. SPIEConf. Ser. Vol. 5489, Ground-based Telescopes. SPIE, Bellingham, p. 679
Steele I. A., Copperwheat C. M., Piascik A. S., 2015, GCN Circ., 18573
Taddia F. et al., 2015, A&A, 574, A60
Taubenberger S. et al., 2006, MNRAS, 371, 1459
Tolstoy E., Hill V., Tosi M., 2009, ARA&A, 47, 371
Tomasella L. et al., 2015a, GCN Circ., 18561
Tomasella L. et al., 2015b, GCN Circ., 18566
Valenti S. et al., 2008a, MNRAS, 383, 1485
Valenti S. et al., 2008b, ApJ, 673, L155
van Eerten H. J., MacFadyen A. I., 2011, ApJ, 733, L37
Walker E. S. et al., 2014, MNRAS, 442, 2768
Walker E. S. et al., 2015, ApJS, 219, 13
Wheeler J. C., Yi I., Höflich P., Wang L., 2000, ApJ, 537, 810
Woosley S. E., Bloom J. S., 2006, ARA&A, 44, 507

This paper has been typeset from a TEX/LATEX file prepared by the author.